Validation of ocean tide models by comparison to gravity loading measurements

O. Francis

Observatoire Royal de Belgique, Avenue Circulaire 3, B-1180 Bruxelles, Belgique
E-mail: francis@astro.oma.be

Introduction

Thanks to the TOPEX/POSEIDON satellite mission, a lot of new ocean tide models are now available. They are claimed to be superior to the Schwiderski model (1980) on the basis of a comparison with 95 selected tides gauges. The Earth Tides community found one's hopes on these new ocean models for improving the loading computations. Nevertheless, most of the new models are not well suited to loading computations because they do not cover the whole oceans and generally they are less reliable over the continental shelves due to the non-linearity of the tides in these areas.

In this short note, we compare the loading computations from two new global ocean tide models with those computed with the Schwiderski model which had been adopted by the Earth Tides community as the working standards. We used the pure hydrodynamic model of Le Provost et al. (1994) so-called the Grenoble model and the adjusted Grenoble model by Andersen (1994) which is an optimal combination of the Grenoble model and TOPEX/POSEIDON altimeter data. As these new models are still subject to improvement, only preliminary versions are available. A main new feature of these models favourable for loading computations is that their resolution is 0.5°x0.5° instead of 1°x1° for the Schwiderski model.

A more detailed comparison with more new ocean tide models will be presented at the IUGG General Assembly in Boulder by Llubes et al. (1995).

Mass conservation.

One of the main grievance of the people concerned by the gravity loading computation against the ocean tide models lies in the fact that they do not generally conserve the mass (Francis, 1992). From Table 1, it is comforting to note that the tidal mass is better conserved in the new models. We can also observe that the models have not only a higher resolution but also they cover more and more oceanic area. For instance, the Andersen includes the Mediterranean. The mean amplitude for the M2 wave is practically unchanged from one model to the other.

In the rest of the computation, I have applied a correction for mass conservation proportional to the tidal amplitude.

Loading computations

In order to calculate the gravity loading effect, the well-known Farrell's method has been used. It consists in evaluating numerically the following convolution integral over the oceans with a kernel, so-called Green's function, which is the response of the earth to a point-like mass load:

$$\mathbb{L}(\phi,\lambda) = \rho_w \iint_{oceans} G(\phi,\lambda;\phi',\lambda')\, \mathbb{h}(\phi',\lambda')\, dS'$$

where L is the gravity loading effect at the geographical location (ϕ,λ), ρ_w is the mean density of the sea water, G the Green's function for the gravitational effect of the load, h ocean tide vector and dS' the surface area. We used the Green's function for an elastic earth using PREM tabulated in Francis and Dehant (1987).

The observed tidal gravity parameters have been taken from the ICET Data Bank containing 352 permanent and temporary stations all around the world which have been recently revised by Melchior (1994). The time series have been analysed using a standard least square adjustment with Venedikov filters. A computed earth model giving the response of the earth to the luni-solar potential is then subtracted from these observations giving the first residue vector $\mathbb{B}(B,\beta)$ (I use the notation introduced in several papers by Melchior). This vector $\mathbb{B}$ contains mainly the oceanic tides contribution to gravity variations. The vector $\mathbb{L}(L,\lambda)$ is the oceanic load vector as calculated from co-range and co-tidal maps. The difference $\mathbb{B}$-$\mathbb{L}$ gives the final residue vector which is the observation noise plus non-modelled contribution.

Comparison between observed residual vector $\mathbb{B}$ and oceanic tidal load $\mathbb{L}$

The coastal stations (distance to the sea less than 10 km) have been discarded because there is disagreement in the computed load vectors when using algorithms from different authors due to the different way of discretizing the convolution integral. My present goal consists in assessing the difference in the ocean tide models and not in the difference in the loading computations in areas where this estimation of the loading is still problematic. I then retain 281 continental tidal gravity stations whose locations are shown in Figure 1.

To compare the observed residual vectors $\mathbb{B}$ with the computed tidal loading vectors $\mathbb{L}$, their cosine and sine components for the M_2 wave are plotted on the same graphs (Figures 2 A-B). The best fit lines are then estimated with the constant values a, the slopes b and the associated mean-square errors (Table 2). The slopes are always higher or equal to 1 for the Grenoble and Andersen models and always lower than 1 for the Schwiderski model. The slope of the sine component for the Grenoble model and of the cosine component for the Andersen model is nearly 1 but this nice correlation is not preserved on the other component. Moreover, I do not observe significant changes in the correlation coefficients which is better for the sine component for all the models as observed previously. The mean-square errors are nearly the same for the cosine components being of the order of 0.56 microgal whereas the mean square errors for the sine components are of the order of 0.35 microgal for the new models i.e. 0.1 microgal less than for the Schwiderski model.

Final Residues $\mathbb{X}$

Histograms of the cosine and sine components for the residual vectors $\mathbb{X}$ are shown in Figures 3 A-B. The Gaussian-like distributions of the residues for the new models are clearly shifted with respect to those calculated with the Schwiderski model. Looking at the standard deviation (Table 3), we observe that there is no improvement for the cosine component whereas for the sine component there is a decrease from 0.7 microgal for the Schwiderski model to 0.6 microgal for the Grenoble and the Andersen models. Nevertheless, there is an anomaly for these models related to the fact that the maxima of the Gaussian-like distributions do not correspond to the average values.

Conclusion

The tidal gravity measurements from the ICET Data Bank contain 'integrated' information on the ocean tides which is independent of the models and then useful for their validation. This work shows slight improvement on gravity loading computations owing to the new global ocean tide models of Grenoble and Andersen: only the standard deviation of the sine component of final residues X for the M_2 wave is slightly reduced. We hoped to improve both components. Before going into further investigations, we will wait for updated solutions of the ocean tide models which should be available soon.

Acknowledgements

I am grateful to Lyard of the Grenoble team and to Andersen for providing me with their ocean tide models. Thanks are also due to Prof. Melchior for reading the manuscript.

References

Andersen, O.B., New Ocean Tide Models for Loading Computations, Bull. Inf. Mar. Terr., this issue, 1995.

Francis, O., Interactions between Earth and Ocean Tides, Bull. Inf. Marées Terrestres, 122, 8131-8144, 1992.

Francis O. and Mazzega P., Global charts of ocean tide loading effects, Journal of Geophysical Research, 95(C7), 11411-11424, 1990.

Le Provost, C. , M.L. Genco, F. Lyard, P. Vincent and P. Canceill, Spectroscopy of the world ocean tides from a finite element hydrodynamical model, J. Geophys. Res., Vol 99, N0. C12, 24777-24797, 1994.

Llubes M., P. Melchior, O. Francis and P. Mazzega, TOPEX/POSEIDON Ocean Tide Models as Compared to the ICET Gravity Data Bank, in preparation, 1995.

Melchior, P., A New data bank for tidal gravity measurements (DB92), Phys. Earth Planet. Inter., 82, 125-155, 1994.

Schwiderski, E.W., Ocean Tides, I, Global ocean tidal equations, Mar. Geod., 3, 161-217, 1980a.

Schwiderski, E.W., Ocean Tides, II; A hydrodynamical interpolation model, Mar. Geod., 3, 219-255, 1980b.

Table 1: Some statistics on the ocean tide models used in this study for the M_2 Wave.

Parameter	Schwiderski	Grenoble	Andersen
Number of grid points	41236	170497	171504
Total surface (m^2)	3.50 10^{+14}	3.57 10^{+14}	3.59 10^{+14}
Mean amplitude (cm)	32.6	33.1	33.2
Residual amplitude (cm)	0.73	0.38	0.07
Ratio Residual /Mean Amplitude	2.2%	1.1%	0.2%

Table 2: Coefficients of the best fit lines (y = a + b x) between observed and computed gravity loading and attraction effects for the M_2 wave.

Parameter	Schwiderski	Grenoble	Andersen
Cosine component			
a (microgal)	-0.03	+0.03	+0.05
b	0.99	1.09	1.00
correlation coefficient	0.71	0.69	0.71
Mean-square error (microgal)	0.56	0.59	0.55
Sine component			
a (microgal)	-0.16	-0.21	-0.22
b	0.95	1.00	1.06
correlation coefficient	0.91	0.91	0.91
Mean-square error	0.49	0.35	0.36

Table 3: Estimated parameters for the histograms of Figures 3.

Parameter	Schwiderski		Grenoble		Andersen	
	Cosine	Sine	Cosine	Sine	Cosine	Sine
Average (microgal)	-0.04	-0.22	-0.08	-0.21	0.05	-0.15
Standard deviation (microgal)	0.75	0.71	0.77	0.59	0.74	0.61
Mimimun value (microgal)	-2.68	-6.27	-3.41	-2.70	-3.24	-2.98
Maximun value (microgal)	4.06	1.74	4.54	2.05	3.85	2.17

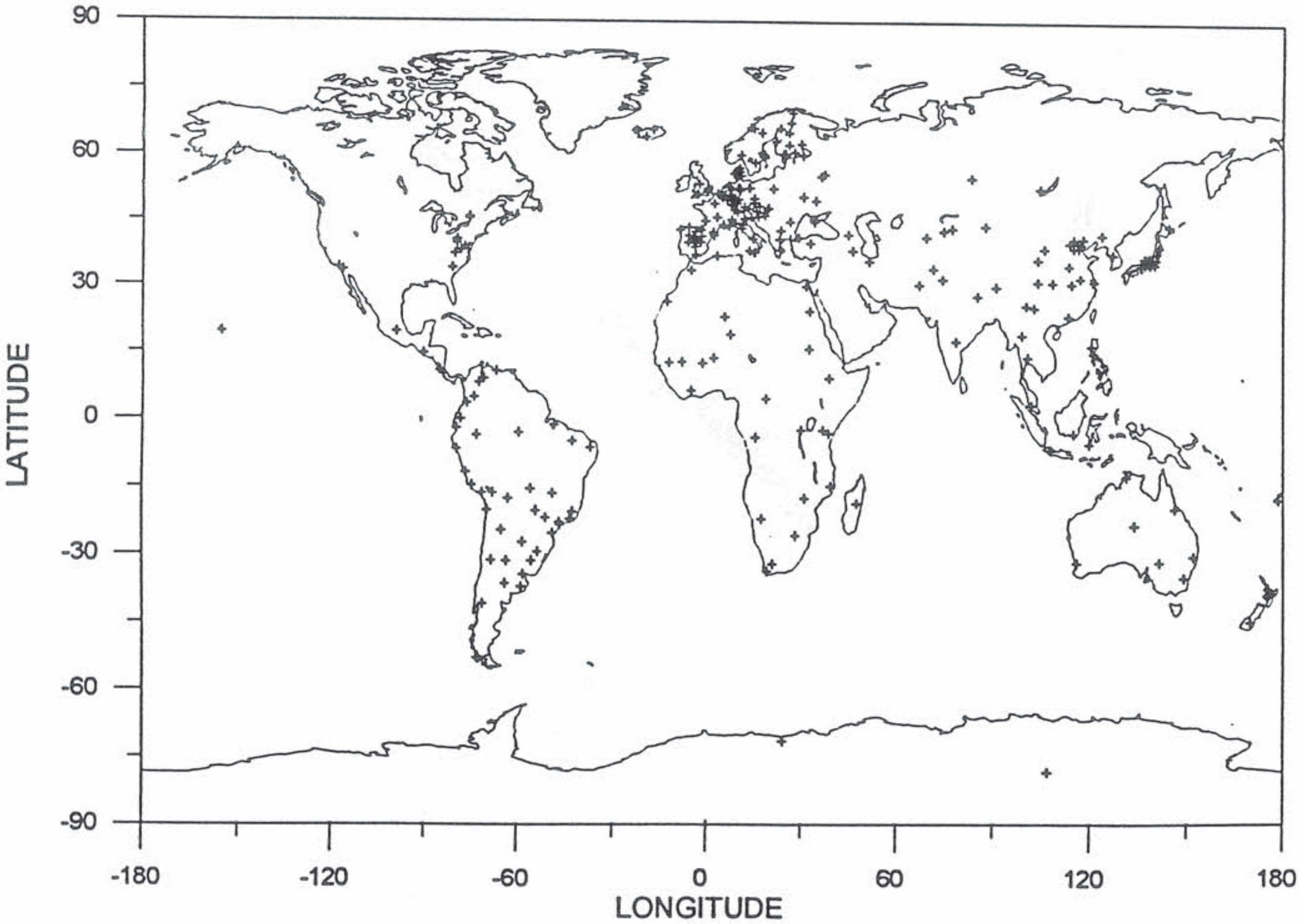

Figure 1: Location of the 281 tidal gravity stations of the ICET Data Bank used for comparison between observed and computed gravity loading effects.

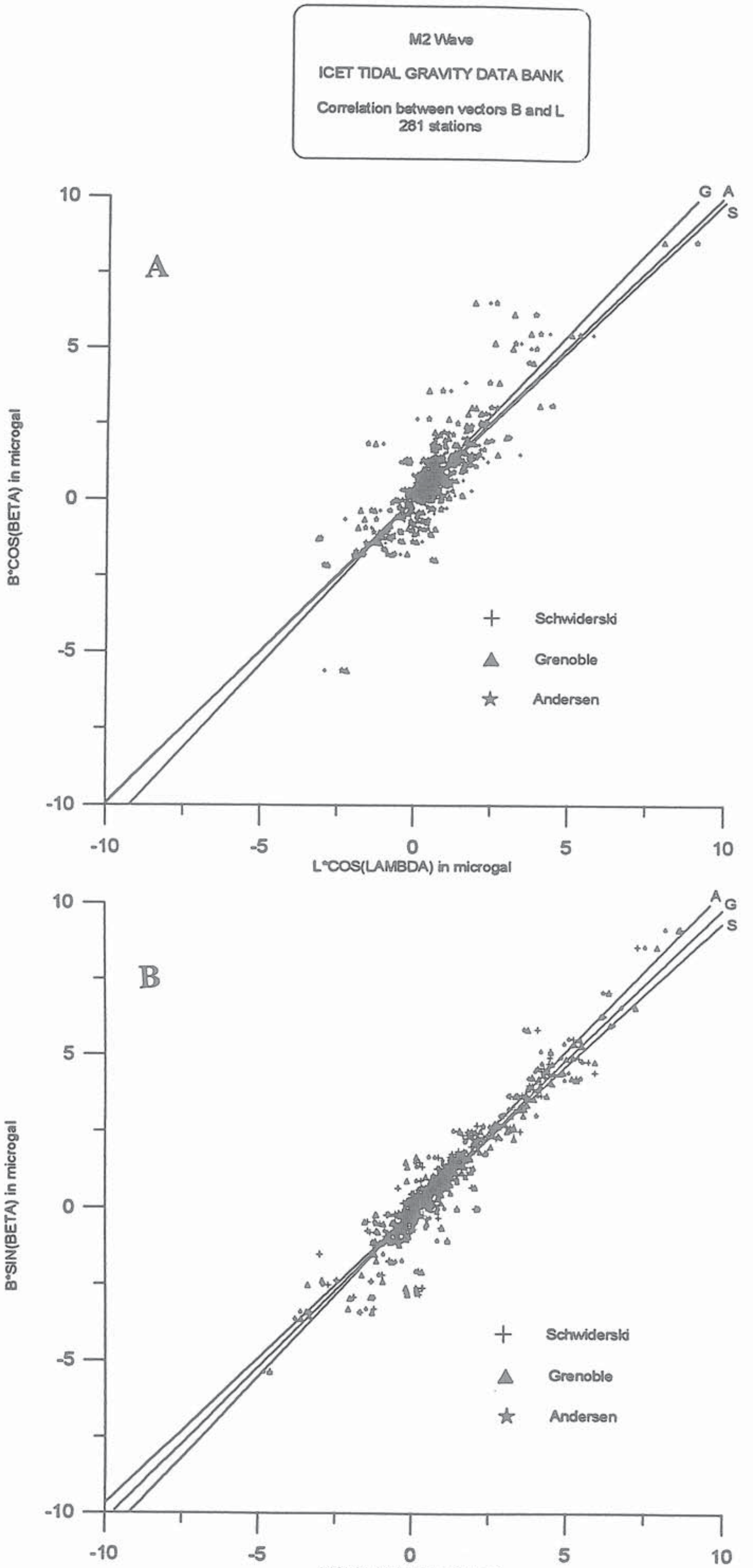

Figures 2: Comparison between observed residual vectors B and computed oceanic loading vectors L for the M_2 wave. (A) Cosine component, (B) Sine component.

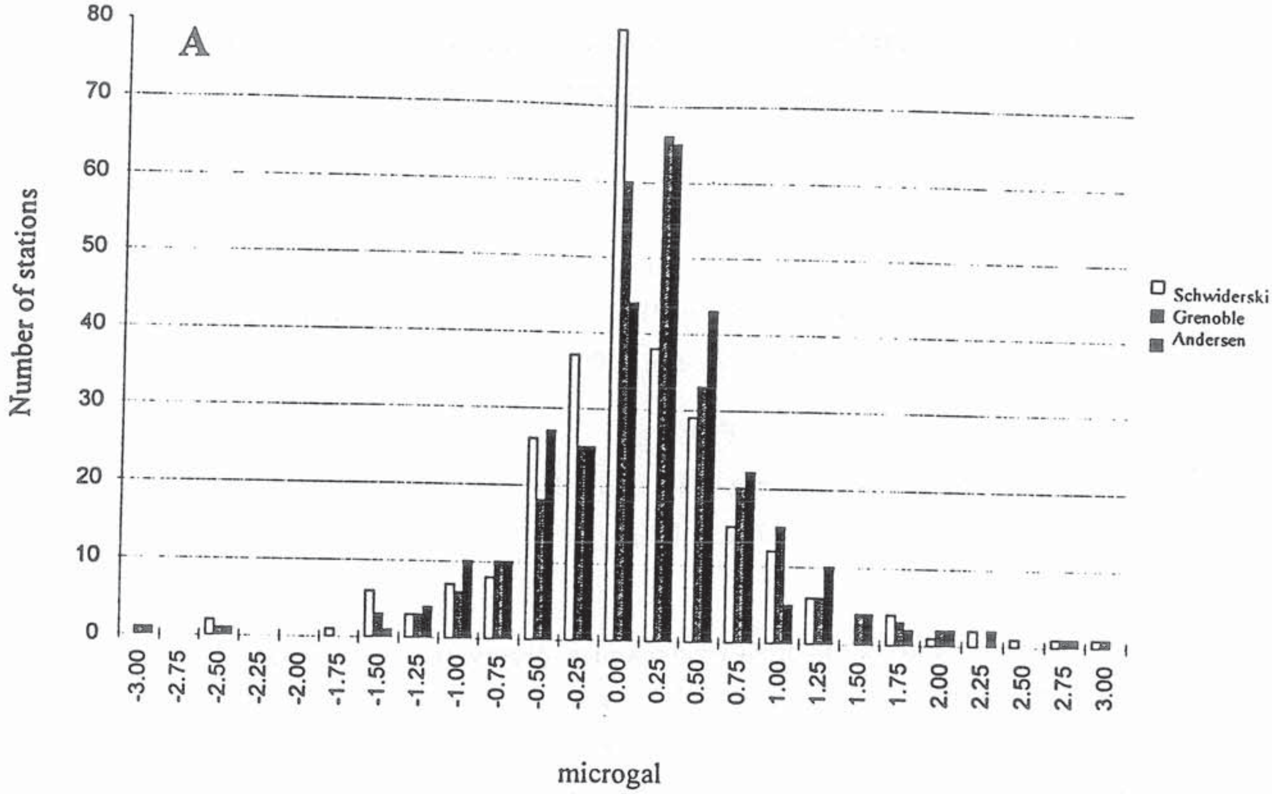

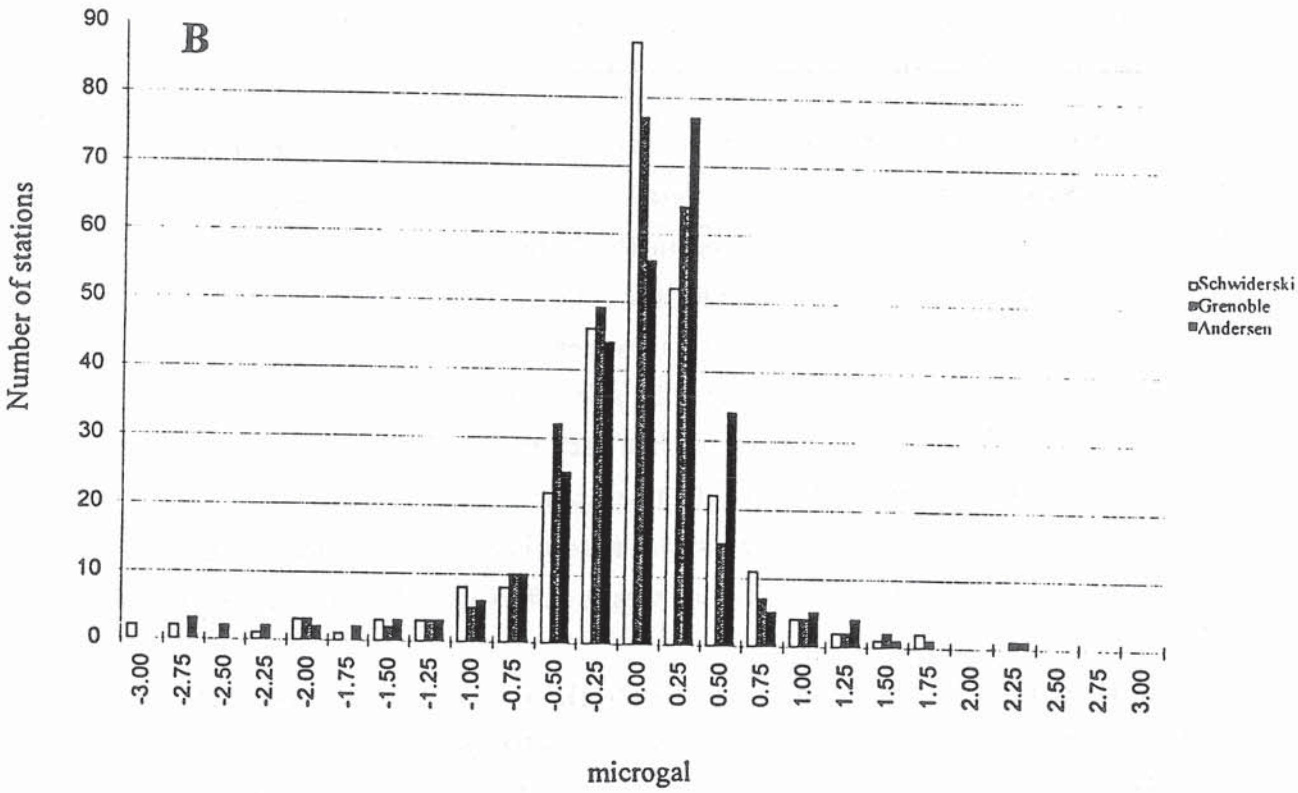

Figures 3: Histograms of the final residues X for the M_2 wave. (A) Cosine component, (B) Sine component.